LETTER

doi:10.1038/nature14296

Orbital-specific mapping of the ligand exchange dynamics of $Fe(CO)_5$ in solution

Ph. Wernet[1], K. Kunnus[1,2], I. Josefsson[3], I. Rajkovic[4]†, W. Quevedo[4]†, M. Beye[1], S. Schreck[1,2], S. Grübel[4]†, M. Scholz[4], D. Nordlund[5], W. Zhang[6]†, R. W. Hartsock[6], W. F. Schlotter[7], J. J. Turner[7], B. Kennedy[8]†, F. Hennies[8], F. M. F. de Groot[9], K. J. Gaffney[6], S. Techert[4,10,11], M. Odelius[3] & A. Föhlisch[1,2]

Transition-metal complexes have long attracted interest for fundamental chemical reactivity studies and possible use in solar energy conversion[1,2]. Electronic excitation, ligand loss from the metal centre, or a combination of both, creates changes in charge and spin density at the metal site[3–11] that need to be controlled to optimize complexes for photocatalytic hydrogen production[8] and selective carbon–hydrogen bond activation[9–11]. An understanding at the molecular level of how transition-metal complexes catalyse reactions, and in particular of the role of the short-lived and reactive intermediate states involved, will be critical for such optimization. However, suitable methods for detailed characterization of electronic excited states have been lacking. Here we show, with the use of X-ray laser-based femtosecond-resolution spectroscopy and advanced quantum chemical theory to probe the reaction dynamics of the benchmark transition-metal complex $Fe(CO)_5$ in solution, that the photo-induced removal of CO generates the 16-electron $Fe(CO)_4$ species, a homogeneous catalyst[12,13] with an electron deficiency at the Fe centre[14,15], in a hitherto unreported excited singlet state that either converts to the triplet ground state or combines with a CO or solvent molecule to regenerate a penta-coordinated Fe species on a sub-picosecond timescale. This finding, which resolves the debate about the relative importance of different spin channels in the photochemistry of $Fe(CO)_5$ (refs 4, 16–20), was made possible by the ability of femtosecond X-ray spectroscopy to probe frontier-orbital interactions with atom specificity. We expect the method to be broadly applicable in the chemical sciences, and to complement approaches that probe structural dynamics in ultrafast processes.

In our experimental setup (Fig. 1a), the valence electronic structure of $Fe(CO)_5$ is probed with femtosecond-resolution resonant inelastic X-ray scattering (RIXS) at the Fe L_3-edge (Fe L_3-RIXS, illustrated in Fig. 1b). The frontier orbitals of ironpentacarbonyl, $Fe(CO)_5$, and its photofragments are the Fe-centred d_π and d_σ* orbitals. With an incident photon energy of 710 eV to select the lowest-energy X-ray resonance corresponding to $2p \rightarrow \mathrm{LUMO}(d_\sigma^*)$ (where LUMO is the lowest unoccupied molecular orbital) excitations and scattering inelastically to the valence-excited ligand-field states with $d_\pi^7 d_\sigma^{*1}$ configuration, we effectively probe $d_\pi \rightarrow d_\sigma^*$ transitions (note that the single-electron orbital-based assignments can be applied at the level that the system is studied here; see Supplementary Information). The energies of these transitions equal the measured energy transfers (that is, the difference between incident and scattered photon energies indicated by 'in' and 'out' in Fig. 1b), and directly reflect the changes in chemical bonding and ligand coordination. The intensities of the transitions in $Fe(CO)_5$ are marked in Fig. 1c (top). The main intensity maximum involves $2p \rightarrow 2\pi^*$ excitations at 711.5 eV with excitation to the ligand-centred $2\pi^*$ orbitals and inelastic scattering to $d_\pi^7 2\pi^{*1}$ charge-transfer states (Fig. 1c) and is not further analysed.

The unsaturated carbonyl $Fe(CO)_4$ was generated in ethanol (EtOH) solution by the photodissociation of $Fe(CO)_5$ with optical (266 nm)

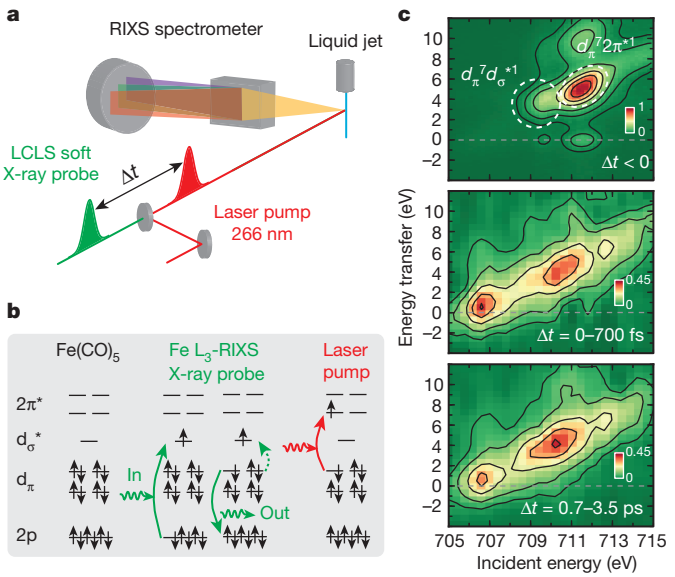

Figure 1 | Scheme and results of the experiment. a, Scheme with optical-laser pump and soft X-ray probe after the pump–probe time delay Δt. The intensity of RIXS is measured at the Fe L_3-absorption edge with a dispersive grating spectrometer. **b**, Electron configuration of ground-state $Fe(CO)_5$ with single-electron transitions of X-ray probe and laser-pump processes (orbital assignments according to Fe 2*p* and 3*d* or ligand 2π character and according to symmetry along the Fe–CO bonds; the asterisk marks antibonding orbitals). RIXS at the Fe L_3-absorption edge with $2p \rightarrow d_\sigma^*$ excitation involves scattering to final $d_\pi^7 d_\sigma^{*1}$ ligand-field excited states. Optical $d_\pi \rightarrow 2\pi^*$ excitation triggers dissociation. **c**, Measured Fe L_3-RIXS intensities (encoded in colour) versus energy transfer and incident photon energy. Top: ground-state $Fe(CO)_5$ (negative delays, probe before pump). Middle and bottom: difference intensities for delay intervals of 0–700 fs and 0.7–3.5 ps, respectively, isolating transients by subtracting scaled intensities of unpumped $Fe(CO)_5$ from the measured intensities (scaling factor 0.9). For details of the experiment and a deduction of the scaling factor see Supplementary Information.

[1]Institute for Methods and Instrumentation for Synchrotron Radiation Research, Helmholtz-Zentrum Berlin für Materialien und Energie GmbH, Albert-Einstein-Strasse 15, 12489 Berlin, Germany. [2]Institut für Physik und Astronomie, Universität Potsdam, Karl-Liebknecht-Strasse 24/25, 14476 Potsdam, Germany. [3]Department of Physics, Stockholm University, AlbaNova University Center, 106 91 Stockholm, Sweden. [4]IFG Structural Dynamics of (bio)chemical Systems, Max Planck Institute for Biophysical Chemistry, Am Fassberg 11, 37077 Göttingen, Germany. [5]Stanford Synchrotron Radiation Lightsource, SLAC National Accelerator Laboratory, 2575 Sand Hill Road, Menlo Park, California 94025, USA. [6]PULSE Institute, SLAC National Accelerator Laboratory, Stanford University, Stanford, California 94305, USA. [7]Linac Coherent Light Source, SLAC National Accelerator Laboratory, Menlo Park, California 94025, USA. [8]MAX-lab, PO Box 118, 221 00 Lund, Sweden. [9]Department of Chemistry, Utrecht University, Universiteitsweg 99, 3584 CG Utrecht, Netherlands. [10]Institute for X-ray Physics, Göttingen University, Friedrich Hund Platz 1, 37077 Göttingen, Germany. [11]Structural Dynamics of (Bio)chemical Systems, DESY, Notkestrasse 85, 22607 Hamburg, Germany. †Present addresses: Paul Scherrer Institut, 5232 Villigen PSI, Switzerland (I.R.); Institute for Methods and Instrumentation for Synchrotron Radiation Research, Helmholtz-Zentrum Berlin für Materialien und Energie GmbH, 12489 Berlin, Germany (W.Q., B.K.); Swiss Light Source, Paul Scherrer Institut, 5232 Villigen PSI, Switzerland (S.G.); Ultrafast Optical Processes Laboratory, Department of Chemistry, University of Pennsylvania, Philadelphia, Pennsylvania 19104, USA (W.Z.).

femtosecond laser pulses in less than 100 fs. Our experiment consisted of recording Fe L_3-RIXS intensities versus energy transfer while scanning incident photon energy and pump–probe time delay with a time resolution of 300 fs. The observed bimodal spectral distribution shows different intensities for different delays (Fig. 1c, middle and bottom), reflecting changes in $2p \rightarrow$LUMO resonance energies within the range 706.5–710 eV and changes in $d_\pi \rightarrow d_\sigma^*$ transition energies within the range −1 to 6 eV. These changes quantify the changes in the frontier-orbital interactions caused by changes in ligand coordination when going from $Fe(CO)_5$ to $Fe(CO)_4$ and during the subsequent excited-state dynamics. Ligand dissociation is expected to create a 'localized hole on the metal'[15] with a concomitant decrease in the d_π–d_σ^* splitting (see the molecular-orbital diagram in Supplementary Information). This manifests itself in the Fe L_3-RIXS spectra at time delays of 0–700 fs (Fig. 1c, middle) as a new $2p \rightarrow$LUMO resonance at 706.5 eV and as the maximum of the $d_\pi \rightarrow d_\sigma^*$ transitions shifted to lower energies by −4 eV relative to $Fe(CO)_5$. Coordinative saturation through ligation with CO or EtOH restores the d_π–d_σ^* splitting, mostly as a result of σ-bonding between $Fe(CO)_4$ and CO or EtOH. This could explain the occurrence of $2p \rightarrow$LUMO and $d_\pi \rightarrow d_\sigma^*$ transition energies comparable to $Fe(CO)_5$ at late delays of 0.7–3.5 ps (at 709.5 and 3 eV; Fig. 1c, bottom).

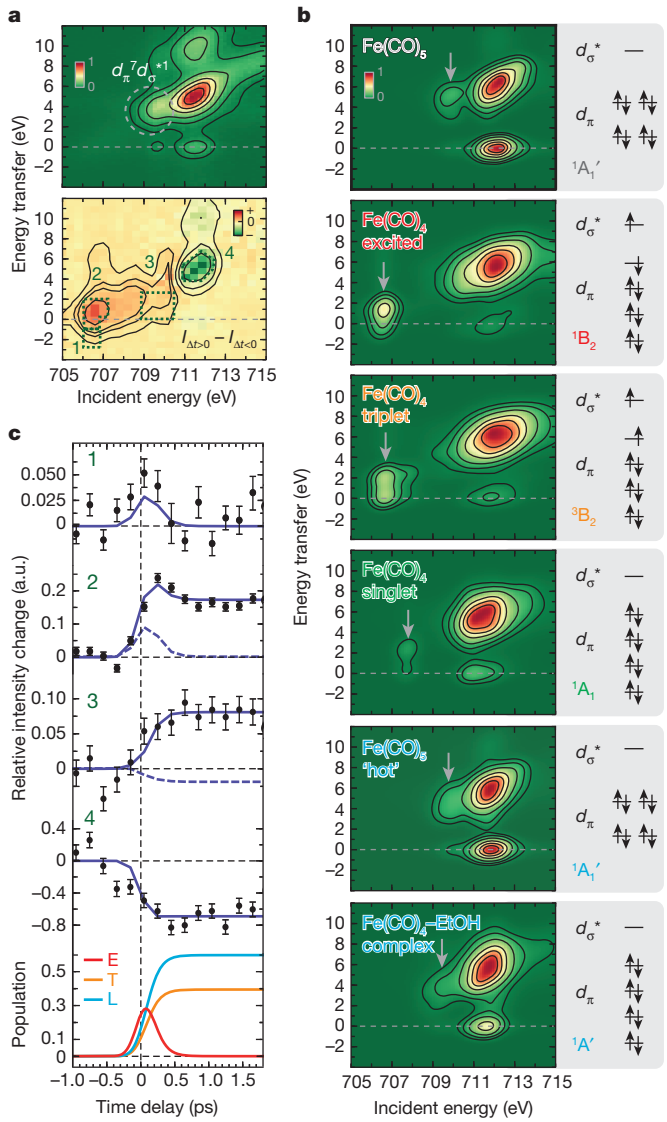

Figure 2 | Fe-specific changes in the electronic structure of $Fe(CO)_4$ after femtosecond spin crossover and ligation. **a**, Measured Fe L_3-RIXS of $Fe(CO)_5$ (top, as in Fig. 1c) and measured difference intensities (bottom, integrated intensities of all positive pump–probe delays minus integrated intensities of all negative delays). The numbers 1–4 mark energy-transfer/incident-photon energy regions for which the temporal evolutions of intensities are plotted in **c**. **b**, Calculated Fe L_3-RIXS intensities and electronic configurations of the given species ($2p \rightarrow$ LUMO and $d_\pi \rightarrow d_\sigma^*$ transitions marked by arrows; the LUMO can be d_σ^* or d_π, depending on the electron configuration). **c**, Plot of measured intensities in regions 1–4 against pump–probe delay (means ± s.d.) with the best global fit of a kinetic model (solid lines) with extracted populations of excited (E), triplet (T) and ligated (L) $Fe(CO)_4$ (L is a sum of 'hot' $Fe(CO)_5$ and $Fe(CO)_4$–EtOH). The dashed lines in regions 2 and 3 represent alternative models without triplet and ligated $Fe(CO)_4$, respectively. The measured signals stayed constant up to 3 ps. For details of the calculations, structures and energies of the species and how ligation in $Fe(CO)_4$–EtOH can occur through the alkyl or hydroxyl group see Supplementary Information.

To substantiate this and to quantitatively analyse the time-resolved data in Fig. 2a, we performed *ab initio* Fe L_3-RIXS calculations for selected structures. The calculated spectra of the three lowest electronic states of $Fe(CO)_4$, of the lowest states of $Fe(CO)_4$–EtOH complexes and of $Fe(CO)_5$ in optimized and distorted geometries account for all experimental features. Figure 2b shows the spectra and electronic configurations corresponding to excited singlet-state $Fe(CO)_4$ ($d_\pi^7 d_\sigma^{*1}$, $^1B_2$), triplet-state $Fe(CO)_4$ ($d_\pi^7 d_\sigma^{*1}$, $^3B_2$), singlet-state $Fe(CO)_4$ ($d_\pi^8 d_\sigma^{*0}$, $^1A_1$), 'hot' singlet $Fe(CO)_5$ ($d_\pi^8 d_\sigma^{*0}$, $^1A_1'$, as represented by structures with distorted geometries compared to the optimized one) and singlet complexes with the solvent $Fe(CO)_4$–EtOH ($d_\pi^8 d_\sigma^{*0}$, $^1A'$).

The most informative spectral regions in our data, labelled 1–4 in Fig. 2a, overlap maximally with the calculated spectral features best able to identify and distinguish the respective intermediate species. The intensities at negative transfers in region 1 result from outgoing X-rays with higher energy than the incoming X-rays and can only result when the X-rays scatter inelastically off $Fe(CO)_4$ fragments in d_π and d_σ^* electronic excited states. Region 2 is dominated by contributions of excited and triplet $Fe(CO)_4$. We emphasize that RIXS gives unique chemical resolution, because integrating over the energy transfer and measuring only time-dependent changes in X-ray absorption would prevent us from distinguishing the dynamics of the species assigned to regions 1 and 2. Region 3 identifies the dynamics of ligated $Fe(CO)_4$ species; that is, $Fe(CO)_5$ and $Fe(CO)_4$–EtOH. Region 4 corresponds to the $2p \rightarrow 2\pi^*$ X-ray resonances with $d_\pi \rightarrow 2\pi^*$ RIXS transitions in most of the calculated species, and seems dominated by the depletion of $Fe(CO)_5$.

The temporal evolution of the Fe L_3-RIXS intensities measured in regions 1–4 is plotted in Fig. 2c, together with the result of a kinetic model that simultaneously fits the sum of the calculated excited-state singlet, triplet and ligated $Fe(CO)_4$ spectra in each region to the measured data (see Supplementary Information for details of the kinetic model and the contribution of singlet $Fe(CO)_4$). This fitting procedure indicates the appearance of the excited singlet state of $Fe(CO)_4$ ($^1B_2$) within the time resolution of our experiment (which is insufficient to resolve the initial, ultraviolet-generated excited state of $Fe(CO)_5$). This allows us to assign unambiguously, within the single-electron orbital picture, the related RIXS intensities at negative energy transfers to $2p \rightarrow d_\pi$ excitations in excited $Fe(CO)_4$ ($d_\pi^7 d_\sigma^{*1}$, $^1B_2$) with predominant inelastic scattering to states with $d_\pi^8 d_\sigma^{*0}$ configuration. As is apparent from the molecular orbital diagram of excited $Fe(CO)_4$ in Fig. 2b, these transitions entail negative energy transfer because the incident photon energy is smaller than the scattered photon energy. The detection and characterization of electronic excited states free from background by non-excited states, enabled by RIXS at negative energy transfers, provides a powerful approach to studying the electronic excited states of chemically active molecules.

The decay of excited singlet-state $Fe(CO)_4$ ($^1B_2$) coincides with the rise of the triplet $Fe(CO)_4$ ground state in solution ($^3B_2$), for which our model gives a time constant of 300 ± 100 fs. Within the experimental uncertainty, our data indicate the simultaneous rise of coordinatively saturated 'hot' $Fe(CO)_5$ arising from geminate recombination with CO and of $Fe(CO)_4$–EtOH arising from complexation with solvent molecules

(fitted time constant 200 ± 100 fs). The failure of kinetic models without triplet $Fe(CO)_4$ ($^3B_2$) (dashed curve in Fig. 2c, region 2) or without ligated $Fe(CO)_4$ (dashed curve in Fig. 2c, region 3) justifies the use of three distinct photoproducts in the kinetic modelling and underlines the robustness of our detection of triplet $Fe(CO)_4$ ($^3B_2$) in parallel with 'hot' $Fe(CO)_5$ and $Fe(CO)_4$–EtOH. Because we cannot spectroscopically distinguish geminately recombined 'hot' $Fe(CO)_5$ from solvent-complexed $Fe(CO)_4$–EtOH, their ratio in the kinetic model is fixed at 1:1, consistent with the measured quantum yield of 0.8 for solvent-separated $Fe(CO)_4$ and CO (ref. 21).

Figure 3 sketches the reaction pathways established in this study, with detection of the excited singlet-state $Fe(CO)_4$ ($^1B_2$) confirming the suggestion[16] that the primary reaction steps in solution also involve the singlet pathway as seen in the gas phase[17,18]. The proposed relaxation of excited singlet $Fe(CO)_4$ ($^1B_2$) to singlet $Fe(CO)_4$ ($^1A_1$) through internal conversion[17] is consistent with our data (see Supplementary Information), but we also observe triplet $Fe(CO)_4$ ($^3B_2$) that was previously seen in solution[4,19] and in rare-gas matrix[16] experiments. This triplet arises from a singlet state with a time constant of 300 fs, consolidating the notion[6] that sub-picosecond intersystem crossing seems to be common in the excited-state dynamics of transition-metal complexes[7,22–24]. The persistence of the triplet $Fe(CO)_4$ ($^3B_2$) up to our maximum time delay of 3 ps is consistent with its undergoing a slow, spin-forbidden reaction with intersystem crossing to a solvent-complexed singlet state on a 50–100 ps timescale[4,5,25]. However, the observed branching on a sub-picosecond timescale into the competing and simultaneous reaction channels of spin crossover and ligation to form coordinatively saturated species introduces an efficient pathway circumventing this spin barrier. It also supports the idea that the high density of electronic excited states and the relatively large amount of excess energy available in the system determine the course of the excited-state dynamics, rather than spin selection rules alone[5,6]. Fast ligation could be facilitated along the singlet pathway, confirming the general notion that solvent-stabilized metal centres form fast[3,4,11]; this is also consistent with the observation of the unsaturated carbonyl $Cr(CO)_5$ forming a solvent complex in alcohol solution within 1.6 ps (ref. 26). An alternative proposal[20] for $Fe(CO)_5$ involves a concerted exchange of CO and EtOH on the timescale of ligand dissociation of 100–150 fs. This would also proceed along a singlet pathway and would be in agreement with our results,

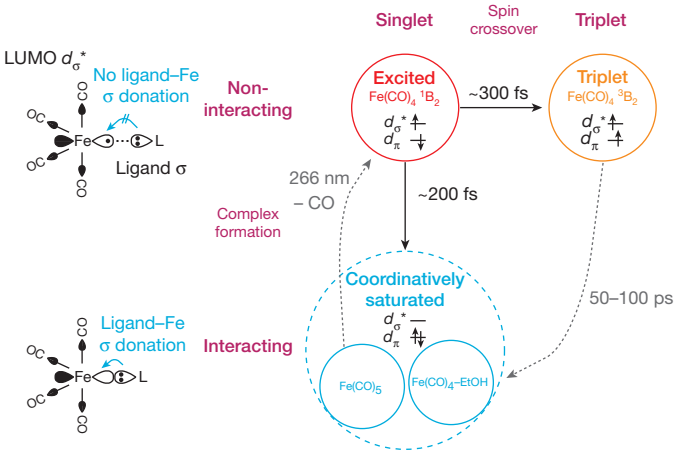

Figure 3 | Schematic reaction pathways of $Fe(CO)_4$ in EtOH. Parallel evolution from excited singlet-state $Fe(CO)_4$ to triplet-state $Fe(CO)_4$ through spin crossover (rise of triplet with a time constant of 300 ± 100 fs) and to coordinatively saturated 'hot' singlet $Fe(CO)_5$ through geminate recombination and $Fe(CO)_4$–EtOH by means of solvent-complex formation (increase in ligated $Fe(CO)_4$ with time constant 200 ± 100 fs). A triplet pathway to $Fe(CO)_4$–EtOH complex formation within 50–100 ps is indicated in grey. Interaction of the d_σ* LUMO of $Fe(CO)_4$ with a ligand σ orbital (different phases are shown in black and white) is shown in the sketches with ligand–Fe σ donation in the coordinatively saturated species.

because the temporal resolution of our measurements is not sufficient to distinguish between this concerted process and the alternative sequential process. Revealing in detail the influence of solvent–solute interactions remains the subject of future studies, which could also explore whether the structure of the solute before dissociation[20] influences the excited-state branching ratio between the different pathways.

We find that the ligation capability of $Fe(CO)_4$ is determined mostly by its d_σ* LUMO, which receives σ donation from occupied CO or EtOH ligand orbitals. Population of the antibonding d_σ* orbital in excited singlet ($^1B_2$) and triplet ($^3B_2$) $Fe(CO)_4$ impedes σ donation from ligands (see the sketches in Fig. 3), explaining the inertness of these species against ligation; this problem is absent in the ligation channel that produces coordinatively saturated species. Establishment of this correlation of orbital symmetry with spin multiplicity and reactivity[27] is enabled by the atom specificity with which X-ray laser-based femtosecond-resolution spectroscopy can explore frontier-orbital interactions. This ability gives unique access to the reaction mechanisms of metal complexes in a way that extends and complements methods that probe structural dynamics in ultrafast chemical processes in solution[28–30].

Received 3 July 2014; accepted 5 February 2015.

1. Parshall, G. W. Organometallic chemistry in homogeneous cata1ysis. *Science* **208,** 1221–1224 (1980).
2. Gray, H. B. & Maverick, A. W. Solar chemistry of metal complexes. *Science* **214,** 1201–1205 (1981).
3. Bengali, A. A., Bergman, R. G. & Moore, C. B. Evidence for the formation of free 16-electron species rather than solvate complexes in the ultraviolet irradiation of $CpCo(CO)_2$ in liquefied noble gas solvents. *J. Am. Chem. Soc.* **117,** 3879–3880 (1995).
4. Snee, P. T., Payne, C. K., Mebane, S. D., Kotz, K. T. & Harris, C. B. Dynamics of photosubstitution reactions of $Fe(CO)_5$: an ultrafast infrared study of high spin reactivity. *J. Am. Chem. Soc.* **123,** 6909–6915 (2001).
5. Besora, M. *et al.* A combined theoretical and experimental study on the role of spin states in the chemistry of $Fe(CO)_5$ photoproducts. *J. Am. Chem. Soc.* **131,** 3583–3592 (2009).
6. Juban, E. A., Smeigh, A. L., Monat, J. E. & McCusker, J. K. Ultrafast dynamics of ligand-field excited states. *Coord. Chem. Rev.* **250,** 1783–1791 (2006).
7. Chergui, M. On the interplay between charge, spin and structural dynamics in transition metal complexes. *Dalton Trans.* **41,** 13022–13029 (2012).
8. Heyduk, A. F. & Nocera, D. G. Hydrogen produced from hydrohalic acid solutions by a two-electron mixed-valence photocatalyst. *Science* **293,** 1639–1641 (2001).
9. Arndtsen, B. A., Bergman, R. G., Mobley, T. A. & Peterson, T. H. Selective intermolecular carbon–hydrogen bond activation by synthetic metal complexes in homogeneous solution. *Acc. Chem. Res.* **28,** 154–162 (1995).
10. Labinger, J. A. & Bercaw, J. E. Understanding and exploiting C–H bond activation. *Nature* **417,** 507–514 (2002).
11. Bromberg, S. E. *et al.* The mechanism of a C–H bond activation reaction in room-temperature alkane solution. *Science* **278,** 260–263 (1997).
12. Wrighton, M. S., Ginley, D. S., Schroeder, M. A. & Morse, D. L. Generation of catalysts by photolysis of transition metal complexes. *Pure Appl. Chem.* **41,** 671–687 (1975).
13. Whetten, R. L., Fu, K.-J. & Grant, E. R. Pulsed-laser photocatalytic isomerization and hydrogenation of olefins. *J. Am. Chem. Soc.* **104,** 4270–4272 (1982).
14. Langmuir, T. Types of valence. *Science* **54,** 59–67 (1921).
15. Hoffmann, R. Building bridges between inorganic and organic chemistry. *Angew. Chem. Int. Edn Engl.* **21,** 711–724 (1982).
16. Poliakoff, M. & Turner, J. J. The structure of $[Fe(CO)_4]$—an important new chapter in a long-running story. *Angew. Chem. Int. Edn Engl.* **40,** 2809–2812 (2001).
17. Trushin, S. A., Fuss, W., Kompa, K. L. & Schmid, W. E. Femtosecond dynamics of $Fe(CO)_5$ photodissociation at 267 nm studied by transient ionization. *J. Phys. Chem. A* **104,** 1997–2006 (2000).
18. Ihee, H., Cao, J. & Zewail, A. H. Ultrafast electron diffraction of transient $[Fe(CO)_4]$: determination of molecular structure and reaction pathway. *Angew. Chem. Int. Edn Engl.* **40,** 1532–1536 (2001).
19. Snee, P. T., Payne, C. K., Kotz, K. T., Yang, H. & Harris, C. B. Triplet organometallic reactivity under ambient conditions: an ultrafast UV pump/IR probe study. *J. Am. Chem. Soc.* **123,** 2255–2264 (2001).
20. Ahr, B. *et al.* Picosecond X-ray absorption measurements of the ligand substitution dynamics of $Fe(CO)_5$ in ethanol. *Phys. Chem. Chem. Phys.* **13,** 5590–5599 (2011).
21. Nayak, S. K., Farrell, G. J. & Burkey, T. J. Photosubstitution of two iron pentacarbonyl CO's in solution via a single-photon process: dependence on dispersed ligands and role of triplet intermediates. *Inorg. Chem.* **33,** 2236–2242 (1994).
22. Zhang, W. *et al.* Tracking excited-state charge and spin dynamics in iron coordination complexes. *Nature* **509,** 345–348 (2014).
23. Bressler, C. *et al.* Femtosecond XANES study of the light-induced spin crossover dynamics in an iron(II) complex. *Science* **323,** 489–492 (2009).
24. Huse, N. *et al.* Femtosecond soft X-ray spectroscopy of solvated transition-metal complexes: deciphering the interplay of electronic and structural dynamics. *J. Phys. Chem. Lett.* **2,** 880–884 (2011).

25. Portius, P. *et al.* Unraveling the photochemistry of $Fe(CO)_5$ in solution: observation of $Fe(CO)_3$ and the conversion between $^3Fe(CO)_4$ and $^1Fe(CO)_4$(solvent). *J. Am. Chem. Soc.* **126,** 10713–10720 (2004).
26. Joly, A. G. & Nelson, K. A. Metal carbonyl photochemistry in organic solvents: femtosecond transient absorption and preliminary resonance Raman spectroscopy. *Chem. Phys.* **152,** 69–82 (1991).
27. Fukui, K. The role of frontier orbitals in chemical reactions. *Angew. Chem. Int. Edn Engl.* **21,** 801–809 (1982).
28. Lim, M., Jackson, T. A. & Anfinrud, P. A. Binding of CO to myoglobin from a heme pocket docking site to form nearly linear Fe–C–O. *Science* **269,** 962–966 (1995).
29. Nibbering, E. T. J., Fidder, H. & Pines, E. Ultrafast chemistry: using time-resolved vibrational spectroscopy for interrogation of structural dynamics. *Annu. Rev. Phys. Chem.* **56,** 338–367 (2005).
30. Greaves, S. J. *et al.* Vibrationally quantum-state-specific reaction dynamics of H atom abstraction by CN radical in solution. *Science* **331,** 1423–1426 (2011).

Supplementary Information is available in the online version of the paper.

Acknowledgements This work was supported by the Volkswagen Stiftung (M.B.) the Swedish Research Council (M.O.), the Carl Tryggers Foundation (M.O.), the Magnus Bergvall Foundation (M.O.), the Collaborative Research Centers SFB 755 and SFB 1073 (I.R., S.G., W.Q., M.S. and S.T.) and the Helmholtz Virtual Institute 'Dynamic Pathways in Multidimensional Landscapes'. W.Z., R.W.H. and K.J.G. acknowledge support through the AMOS program within the Chemical Sciences, Geosciences, and Biosciences Division of the Office of Basic Energy Sciences, Office of Science, US Department of Energy. Portions of this research were performed on the Soft X-ray Materials Science (SXR) Instrument at the Linac Coherent Light Source (LCLS), a division of SLAC National Accelerator Laboratory and an Office of Science user facility operated by Stanford University for the US Department of Energy. The SXR Instrument is funded by a consortium whose membership includes the LCLS, Stanford University through the Stanford Institute for Materials Energy Sciences (SIMES), Lawrence Berkeley National Laboratory (LBNL), the University of Hamburg through the BMBF priority program FSP 301, and the Center for Free Electron Laser Science (CFEL).

Author Contributions Ph.W., K.K., I.R., W.Q., M.B., S.S., D.N., W.F.S., J.J.T., F.H., S.T. and A.F. designed the experiment. Ph.W., K.K., I.R., W.Q., M.B., S.S., S.G., M.S., D.N., W.Z., R.W.H., W.F.S., J.J.T., B.K., F.H., K.J.G., S.T. and A.F. did the experiment. K.K., Ph.W., M.B. and A.F. analysed the experimental data. I.J., K.K. and M.O. performed the calculations. Ph.W., K.K. and K.J.G. wrote the manuscript with input from all authors.

Author Information Reprints and permissions information is available at www.nature.com/reprints. The authors declare no competing financial interests. Readers are welcome to comment on the online version of the paper. Correspondence and requests for materials should be addressed to Ph.W. (wernet@helmholtz-berlin.de), M.O. (odelius@fysik.su.se) or A.F. (alexander.foehlisch@helmholtz-berlin.de).